

# Spin-lattice relaxation of the nuclear magnetic system of a solid with multispin interactions induced by a modulated strong rf field

V. E. Zobov

*L. V. Kirenskiĭ Institute of Physics, Russian Academy of Sciences, Siberian Branch,  
660036 Krasnoyarsk, Russia*

M. A. Popov

*Krasnoyarsk State University, 660041 Krasnoyarsk, Russia*

(Submitted 19 January 1996)

*Zh. Éksp. Teor. Fiz.* **110**, 635–660 (August 1996)

When a NMR line of a solid narrows at the “magic” orientation of the effective field in the rotating frame, the linewidth is determined by a three-spin effective interaction, rather than by the original dipolar interaction. When the line is narrowed further by a second effective field acting in the doubly rotating reference frame, the spin dynamics are now determined by four- and five-spin effective interactions. The Hamiltonian for these interactions is found. An expression for the longitudinal nuclear spin-lattice relaxation time in the third effective field acting in the triply rotating reference frame is found. This expression consists of terms with two-, three-, four-, and five-particle correlation functions of products of the dipolar coupling constants modulated by the atomic and molecular motions. The dependence of this time on the correlation frequencies of the motions is calculated in the approximation of high-dimensionality lattices for different models of the motion and values of the rf field parameters. The high sensitivity of the spin-lattice relaxation time in the triply rotating frame to details of the ultraslow internal motions in the solid is demonstrated; measuring it can therefore provide an effective way to investigate such motions. A method is proposed for testing the correlation of the atomic motions directly by comparing experimental plots of the temperature dependence of two- and three-spin relaxations measured when the first and second effective fields, respectively, deviate from their “magic” orientations. © 1996 American Institute of Physics.  
[S1063-7761(96)02008-2]

## 1. INTRODUCTION

Investigating nuclear spin-lattice relaxation is a generally accepted method for studying atomic and molecular motions in solids.<sup>1</sup> The traditional nuclear magnetic resonance (NMR) methods measure the spin-lattice relaxation time of the magnetization in a strong constant field ( $T_1$ ) or in a radio-frequency (rf) field in a rotating reference frame ( $T_{1\rho}$ ). Each motion appears in the expressions for these times in terms of the Fourier transform of the temporal two-particle correlation function of the dipolar coupling constants at the precession frequency in the corresponding field. The calculation of the relaxation times and the analysis of the relaxation curves are significantly simpler than the calculation and analysis of the NMR line shape of the dense spin system in a solid. However, the line shape is more sensitive to details of the motions of atoms and molecules, since it is actually determined by many-particle correlation functions of products of the dipolar coupling constants of from two to an infinite number of particles.

The modern methods of NMR spectroscopy<sup>2,3</sup> based on the effects of a pulsed or continuous strong rf field on the nuclear spin system make it possible to combine the simplicity of the relaxation methods with the informativeness of the spectral methods. In fact, under the action of an rf field that is strong compared with the dipolar interaction, the dynamics of the spin system is determined not by the original two-spin

interaction, but by an effective multispin interaction,<sup>2–4</sup> the number of spins participating in an elementary event increasing as the form of the applied rf field becomes more complicated. Therefore, it becomes possible<sup>5–7</sup> to selectively observe the correlation functions of dipolar coupling constants with an assigned number of particles, viz., two, three, four, or more, using the spin-lattice relaxation time. An analysis of plots of the temperature dependence of such a multiple-frequency spin-lattice relaxation time permits determination not only of the rates, but also of the types of atomic and molecular motions. Also, since the effective interaction is many times weaker than the original interaction, it is specifically the ultraslow motions characteristic of the solid phase that will be accessible to study.

The method described has not attracted the attention it should from investigators. The amount of information obtained is increased by employing the modern methods of two-dimensional or multiple-quantum NMR spectroscopy,<sup>3,8</sup> in which active treatment of the spectrum simplifies its analysis. For example, such a fine characteristic of molecular motion as correlation was found from multiple-quantum spectra in Ref. 9. The analysis of a spectrum can be simplified if the number of magnetic nuclei in the molecule or in the molecular group studied is not excessively large. Since this is not the case in the dense nuclear spin system of a crystal, the spectrum does not become simpler than the original one after it has been separated according to the chemical

shifts or when multiple-quantum transitions are observed.<sup>10</sup> In such systems the method described above of measuring many-particle spin-lattice relaxation is the only way remaining to extract detailed information on the internal mobility.

Spin-lattice relaxation caused by a three-spin effective interaction was observed experimentally in Ref. 11. Under the conditions of that experiment a strong continuous rf field that forms an effective field having the "magic" orientation in a rotating frame<sup>4</sup> acted on the nuclear spin system of solid benzene. The shallow modulation of the rf field in a doubly rotating frame (the second rotation is about the effective field) created a second effective field. The relaxation time ( $T_{1\rho\rho}$ ) of the magnetization directed along this field was measured. The method employed of directly recording NMR in the rotating frame, which was developed by Mefed *et al.*,<sup>12-14</sup> has several advantages over the method of multiple-pulse sequences and ensured the success of the experiment. Mefed<sup>15</sup> recently showed how the longitudinal spin-lattice relaxation time ( $T_{1\rho\rho\rho}$ ) of the magnetization parallel to the third effective field in a triply rotating frame (the third rotation is about the second field) can be measured by direct recording. The time  $T_{1\rho\rho\rho}$  is governed already by four- and five-spin effective interactions.

The purpose of the present work is to develop the theory needed for the successful practical implementation of this method for studying motions on the basis of the multiple-particle spin-lattice relaxation time. General equations for  $T_{1\rho}$  (Refs. 1 and 2) and  $T_{1\rho\rho}$  (Refs. 6 and 7) are presently known. There are no equations for  $T_{1\rho\rho\rho}$ ; they are derived in this paper. For this purpose in the third and fourth sections, respectively, four- and five-spin effective Hamiltonians are found and divided into parts that are nonsecular toward the third field, which are used to obtain the equations sought in second-order time-dependent perturbation theory. Then the dependence of  $T_{1\rho\rho\rho}$  on the motional correlation frequency is calculated for various cases in the fifth section. The influence of the motion model, nonuniformity of the rf field, and deviations of the first and second effective fields from their magic orientations is analyzed. Finally, the coefficients needed for the calculations in the approximation of lattices of large dimensionality are calculated in the Appendix.

## 2. NUCLEAR SPIN SYSTEM IN A MODULATED rf FIELD

Consider the system of nuclear spins ( $I = 1/2$ ) of a crystal in a strong constant magnetic field  $H_0$  and a strong transverse rf field with amplitude  $2H_1$  and frequency  $\omega$ , which is close to the Larmor precession frequency  $\omega_0 = \gamma H_0$  and is modulated in the following manner:<sup>15,16</sup>

$$H_1(t) = 2H_1 \cos\{\omega t + \varphi + \delta\varphi \cos[\Omega_1 t + \delta\varphi_1 \times \cos(\Omega_2 t + \varphi_2)]\}, \quad (2.1)$$

where  $\{\delta\varphi, \delta\varphi_1\} \ll \pi/2$ .

At first we set  $\delta\varphi = 0$ . In the reference frame rotating with the frequency  $\omega$  about the field  $H_0$ , an effective field<sup>4</sup> of strength  $\omega_e$  (in frequency units), which forms an angle  $\theta$  with the field  $H_0$ , acts on the spins:

$$\omega_e = [\gamma^2 H_1^2 + (\omega - \omega_0)^2]^{1/2}, \quad \theta = \arctan[\gamma H_1 / (\omega_0 - \omega)].$$

When the rf field is nonuniform,  $H_1$  and  $\omega_e$  are understood to be their transform-averaged values  $\bar{H}_1$  and  $\bar{\omega}_e$ , and the deviation is taken into account by a correction term in the Hamiltonian (here and in the following we measure the energy in frequency units):

$$\mathcal{H}_{\text{rf}} = -\omega_e \sin\theta \sum_i \eta_i [I_i^x \cos\theta + I_i^z \sin\theta], \quad (2.2)$$

where  $\{I_i^x, I_i^y, I_i^z\}$  are the components of the spin vector operator at the site  $i$  in the reference frame with the  $z$  axis parallel to the effective field  $\omega_e$ , and  $\eta_i = H_{1i} / \bar{H}_1 - 1$ . For example, under the experimental conditions in Refs. 11–16 the degree of nonuniformity is estimated to be 0.15%.

We write the Hamiltonian of the system in the rotating frame in the following manner:

$$\mathcal{H} = -\omega_e I_z + \sum_{m=0, \pm 1, \pm 2} \mathcal{H}^m, \quad I_z = \sum_i I_i^z, \quad (2.3)$$

where, besides the Zeeman interaction in the effective field, we have separated the parts that satisfy the condition

$$[I_z, \mathcal{H}^m] = m \mathcal{H}^m. \quad (2.4)$$

The secular part is

$$\begin{aligned} \mathcal{H}^0 = & -\omega_e \sin^2\theta \sum_i \eta_i I_i^z + \frac{1}{2}(3\cos^2\theta - 1) \\ & \times \sum_{i \neq j} b_{ij} \left[ I_i^z I_j^z - \frac{I_i^x I_j^x + I_i^y I_j^y}{2} \right], \end{aligned} \quad (2.5)$$

where  $b_{ij} = \gamma^2 \hbar [1 - 3\cos^2(\theta_{ij})] 2r_{ij}^3$ , and  $\theta_{ij}$  is the angle between the internuclear vector  $r_{ij}$  and the constant magnetic field  $H_0$ . The contribution for the dipolar interaction to (2.5) vanishes at the magic angle  $\theta = \theta_M = 54.74^\circ$  (Ref. 4). At that angle, for the nonsecular parts in (2.3) we obtain

$$\mathcal{H}^{\pm 1} = -\frac{\sqrt{2}}{6} \omega_e \sum_i \eta_i I_i^{\pm} - \frac{1}{\sqrt{2}} \sum_{i \neq j} b_{ij} I_i^z I_j^{\pm}, \quad (2.6)$$

$$\mathcal{H}^{\pm 2} = \frac{1}{4} \sum_{i \neq j} b_{ij} I_i^{\pm} I_j^{\pm}, \quad I_i^{\pm} = I_i^x \pm I_i^y.$$

Under the action of the effective field the nonsecular parts  $\mathcal{H}^m$  ( $m \neq 0$ ) oscillate rapidly with time at the frequencies  $m\omega_e$ . Their contribution to the slow relaxation processes in the spin system can be taken into account by means of the theory of averaging in terms of the effective Hamiltonian<sup>4,7</sup>

$$\mathcal{H}_{\text{eff}} = \mathcal{H}_{\text{eff}}^{(3)} + \mathcal{H}_{\text{eff}}^{(4)} + \dots, \quad (2.7)$$

where

$$\mathcal{H}_{\text{eff}}^{(3)} = \frac{1}{2\omega_e} \sum_{m=\pm 1, \pm 2} [\mathcal{H}^{-m}, \mathcal{H}^m] / m, \quad (2.8)$$

$$\begin{aligned} \mathcal{H}_{\text{eff}}^{(4)} = & \frac{1}{2\omega_e^2} \{ [\mathcal{H}^{\pm 1}, [\mathcal{H}^{\pm 1}, \mathcal{H}^{\pm 2}]] \\ & + [\mathcal{H}^{-1}, [\mathcal{H}^{-1}, \mathcal{H}^{\pm 2}]] \} \end{aligned} \quad (2.9)$$

are the first two terms of the series. The ratio of the local field to the effective field is actually a small parameter. Rather than the root-mean-square value of the local field ( $H_L$ ), it is more convenient to use the second moment of the NMR absorption line, which is related to it by the simple expression

$$M_{2d} = \frac{9}{4N} \sum_{i,j} b_{ij}^2 = 3H_L^2,$$

where  $N$  is the number of spins in the system and the small parameter is

$$\varepsilon = (M_{2d}/\omega_e^2)^{1/2}.$$

In turn, we characterize the effective interaction by the second moment of the NMR line in the rotating frame  $M_{2\rho}$  (Refs. 12–14).

We turn to the general case (2.1). Confining ourselves to the first order in the expansion of this expression in the small parameter  $\delta\varphi$ , in the rotating frame we obtain an additional term in the Hamiltonian:

$$\begin{aligned} \mathcal{H}'_{\text{eff}} = & 2\gamma H_2 \cos[\Omega_1 t + \varphi_1 + \delta\varphi_1 \cos(\Omega_2 t + \varphi_2)] \\ & \times \sum_i (1 + \eta_i) I_i^y, \end{aligned} \quad (2.10)$$

where  $H_2 = H_1 \delta\varphi/2$ . We now move on to the doubly rotating frame spinning with a frequency  $\Omega_1$  about the effective field. For simplicity, let  $\delta\varphi_1 = 0$ . Then a second effective field<sup>11–16</sup> of strength  $\omega_2$  (in frequency units), which forms an angle  $\theta'$  with the field  $\omega_e$ , acts on the spins in this reference frame:

$$\begin{aligned} \omega_2 = & [(\gamma H_2)^2 + (\Omega_1 - \omega_e)^2]^{1/2}, \\ \theta' = & \arctan[\gamma H_2 / (\omega_e - \Omega_1)]. \end{aligned} \quad (2.11)$$

When the second field has sufficient strength ( $\omega_2 \gg M_{2\rho}^{1/2}$ ), it causes fast oscillations of the effective Hamiltonian (2.7) and thereby leads to further weakening of the effective interaction. The greatest narrowing of the NMR line of a solid<sup>13,14</sup> is achieved when the second effective field is orthogonal to the first. Under these conditions the parts of  $\mathcal{H}'_{\text{eff}}{}^{(3)}$  given by (2.8) and the contribution from the nonuniformity of the rf field to (2.5) that are secular in the second field vanish. Therefore, the dynamics of the spin system is determined by the weaker new effective interaction ( $\mathcal{H}'_{\text{eff}}{}^{(5)}$ ) formed according to the same rule (2.8) (with the replacement of  $\omega_e$  by  $\omega_2$ ), but now from the parts of the effective Hamiltonian  $\mathcal{H}'_{\text{eff}}{}^{(3)}$  that are nonsecular and satisfy the property (2.4) with respect to the second field (Ref. 7) and Eq. (2.5):

$$\mathcal{H}'_{\text{eff}}{}^{\pm 1} = \xi \sum_{i \neq j \neq k} \{ \zeta_{k,ij} I_k^{\pm} I_i^{\pm} I_j^{\pm} + \alpha_{k,ij} I_k^{\mp} I_i^{\pm} I_j^{\pm} \} + \xi \sum_i \Delta_i I_i^{\pm}, \quad (2.12)$$

$$\mathcal{H}'_{\text{eff}}{}^{\pm 3} = \xi \sum_{i \neq j \neq k} \beta_{ijk} I_i^{\pm} I_j^{\pm} I_k^{\pm},$$

where

$$\begin{aligned} \zeta_{k,ij} = & 4(b_{ik}b_{kj} - 2b_{ij}b_{jk} - 2b_{ji}b_{ik}), \\ \alpha_{k,ij} = & (5b_{ij}b_{jk} + 5b_{ji}b_{ik} - b_{ik}b_{kj}), \\ \beta_{ijk} = & 7(b_{ij}b_{jk} + b_{ik}b_{kj} + b_{ji}b_{ik})/3, \end{aligned} \quad (2.13)$$

$$\Delta_i = 6 \sum_{j(\neq i)} b_{ij}^2 + \frac{32\omega_e^2 \eta_i}{3}, \quad \xi = -\frac{1}{32\omega_e},$$

and the  $z$  axis is directed along the second field. The Hamiltonian  $\mathcal{H}'_{\text{eff}}{}^{(5)}$  is second-order in  $\varepsilon$  and will be found in the fourth section of this paper. The part of the effective Hamiltonian that is of the same order  $\varepsilon$  and secular in the second field is  $\mathcal{H}'_{\text{eff}}{}^{(4)}$  given by (2.9), which will be found in the third section of this paper.

In addition, the Hamiltonian contains a term due to the nonuniformity of the second field in (2.10). Since the rf field scarcely varies on the scales of atomic and molecular motions, this term does not make a contribution to the spin-lattice relaxation. However, it makes a contribution to the residual NMR linewidth<sup>14</sup> that is quite appreciable in a liquid. It can be balanced<sup>14</sup> by the contribution from the nonuniformity of the rf field to (2.5), if we take the angle  $\theta'$  specified by equating the projections of the two contributions onto the second field:

$$\gamma H_2 \sin\theta' + \omega_e \sin^2\theta \cos\theta' = 0,$$

whence follows  $\theta' \approx \pi/2 + \gamma H_2 / \omega_e \sin^2\theta$  for  $\gamma H_2 \ll \omega_e \sin^2\theta$ .

Finally, when we have  $\delta\varphi_1 \neq 0$  in (2.10), going over to the triply rotating frame (the third rotation is about the second field with a frequency  $\Omega_2 = \omega_2$ ), we obtain a third effective field<sup>14,15</sup> of strength (in frequency units)

$$\omega_3 = \frac{1}{4} \gamma H_1 \delta\varphi \delta\varphi_1,$$

which is orthogonal to the second. Note that to be specific we chose phase modulation of the rf field<sup>15,16</sup> above in (2.1). The results obtained in the present work are equally applicable to other types of modulation,<sup>11–14</sup> viz., amplitude and frequency modulation. Only the equations defining  $H_2$  and  $\omega_3$  change.

Under the conditions of the experiment in Ref. 15 the phases  $\varphi_1$  and  $\varphi_2$  are chosen so that at  $t=0$  the second field is orthogonal to  $H_0$  and the third field is parallel to  $H_0$ . The magnetization is captured by the third field (spin locking in the triply rotating reference frame) and follows it without significant losses, if the third field is sufficiently large relative to the effective interaction in the triply rotating frame, whose magnitude will be characterized by the second moment of the NMR line in the doubly rotating frame  $M_{2\rho\rho}$ ,<sup>13,14</sup> i.e., if  $\omega_3 > M_{2\rho\rho}^{1/2}$ . The conditions for spin locking in a triply rotating frame are similar to those in a doubly rotating frame, studied in Refs. 11, 14, and 16. In a rigid lattice the projection of the magnetization onto the third field

should not vary with time. When there is atomic and molecular mobility, relaxation of this magnetization is observed under the action of the parts of the effective Hamiltonian  $\mathcal{H}_{ee}^m$  that are nonsecular in the third field and satisfy the condition (2.4) with respect to that field. For the longitudinal spin-lattice relaxation rate in the case under consideration, from time-dependent perturbation theory<sup>2,5-7,17</sup> we obtain the relation

$$\frac{1}{T_{1\rho\rho\rho}} = 2 \sum_{m=1}^5 m^2 J_m(m\omega_3), \quad (2.14)$$

where  $J_m(\omega)$  is the Fourier transform of the correlation function

$$G_m(t) = \langle \text{Tr} \{ \mathcal{H}_{ee}^m(t) \mathcal{H}_{ee}^m(0) \} \rangle / \text{Tr} \{ I_z^2 \}, \quad (2.15)$$

in which the averaging is carried out over the random motions of the atoms and molecules in the coordinate space. We note that if  $\mathcal{H}_{ee}^m$  has a part  $\langle \mathcal{H}_{ee}^m \rangle$  that is conserved during motion and does not make a contribution to the spin-lattice relaxation,  $\text{Tr} \{ \langle \mathcal{H}_{ee}^m \rangle \langle \mathcal{H}_{ee}^m \rangle \} / \text{Tr} \{ I_z^2 \}$  should be subtracted from the right-hand side of (2.15).

### 3. CONTRIBUTION OF THE SECOND-ORDER EFFECTIVE HAMILTONIAN $\mathcal{H}_{\text{eff}}^{(2)}$ TO THE SPIN-LATTICE RELAXATION

After calculating the commutators in (2.9), for the Hamiltonian sought we find

$$\begin{aligned} \mathcal{H}_{\text{eff}}^{(4)} = & \frac{1}{\omega_e^2} \sum \left\{ b_{ik} b_{kj} b_{jl} I_i^z I_j^z I_k^z I_l^z + \frac{1}{2} \left[ b_{ki} b_{ij} (b_{jl} - b_{kl}) \right. \right. \\ & + \left. \frac{b_{ij} b_{ik} b_{il}}{2} \right] (I_i^x I_k^x + I_j^y I_l^y) (I_j^x I_i^x + I_j^y I_l^y) - \left[ b_{ki} b_{ij} b_{jl} \right. \\ & + \left. \frac{1}{2} (b_{kl} b_{li} b_{ij} + b_{ij} b_{ik} b_{il} + b_{lk} b_{lj} b_{li}) \right] I_i^z I_k^z (I_j^x I_l^x \\ & + I_j^y I_l^y) \left. \right\} + \frac{1}{4\omega_e^2} \sum A_{ij} \left[ I_i^z I_j^z - \frac{I_i^x I_j^x + I_i^y I_j^y}{2} \right], \quad (3.1) \end{aligned}$$

where

$$\begin{aligned} A_{ij} = & \sum_{k(\neq\{i,j\})} \left\{ b_{ik} b_{kj} b_{ji} + \frac{1}{2} [b_{ik} b_{kj}^2 + b_{ik}^2 b_{kj} \right. \\ & \left. - (b_{ik}^2 + b_{jk}^2) b_{ij}] \right\}. \end{aligned}$$

In (3.1) and in similar equations below the summation is carried out over all the lattice indices appearing in them under the condition that terms with two identical indices are excluded.

To calculate the contribution of this Hamiltonian to the longitudinal spin-lattice relaxation in the third field (2.14), in (3.1) we isolate the part that is secular in the second field, from which we then isolate the parts that are nonsecular in the third field and satisfy the condition (2.4):

$$\begin{aligned} \mathcal{H}_{ee1}^{+2} &= -48\xi^2 \sum I_i^+ I_j^+ A_{ij}, \\ \mathcal{H}_{ee2}^{+2} &= -24\xi^2 \sum I_j^z I_i^z I_k^+ I_l^+ \left\{ 2|i, \overline{jkl}| + 12(\overline{ijkl}) + 8(\overline{jikl}) - 8(\overline{kijl}) \right\}, \\ \mathcal{H}_{ee3}^{+2} &= 6\xi^2 \sum I_i^- I_k^+ I_j^+ I_l^+ \left\{ 12|i, \overline{jkl}| - 8(\overline{ijkl}) \right\}, \\ \mathcal{H}_{ee}^{+4} &= 30\xi^2 \sum I_i^+ I_k^+ I_j^+ I_l^+ \left\{ |i, \overline{jkl}| + 2(\overline{ijkl}) \right\}. \end{aligned} \quad (3.2)$$

Here the  $z$  axis is parallel to the third field, and the following symbolic notation is introduced for the products of the dipolar coefficients:

$$(ijkl) = b_{ij} b_{jk} b_{kl}, \quad |i, jkl| = b_{ij} b_{ik} b_{il}. \quad (3.3)$$

The joining of the lattice indices in the coefficients in (3.2) by lines schematically denotes their symmetrization with respect to the interchange of these indices in the products (3.3):

$$\begin{aligned} 4|\overline{i, jkl}| &= |i, jkl| + |j, ikl| + |k, ij| + |l, ijk|, \\ 12(\overline{ijkl}) &= (ijkl) + (ikjl) + (iklj) + (iljk) + (ilkj) + (ijlk) \\ &+ (klij) + (kjil) + (kijl) + (kilj) + (jikl) + (jkil), \\ 4(\overline{jikl}) - 4(\overline{kijl}) &= (jikl) + (jkil) + (klji) + (kjli) \\ &- (kijl) - (ikjl) - (kilj) - (iklj). \end{aligned} \quad (3.4)$$

Such symmetrization enables us to obtain more compact expressions and to simplify the calculations of the traces in (2.15). The Hermitian conjugate parts  $\mathcal{H}_{ee}^2$  and  $\mathcal{H}_{ee}^4$  of the Hamiltonian are obtained after the replacement of  $I^+$  by  $I^-$  and of  $I^-$  by  $I^+$  in (3.2).

The substitution of (3.2) into (2.15) gives correlation functions of products of the dipolar coefficients of different kinds, which we shall represent using graphical expressions: the lattice sites (spins) are depicted by circles, and the interactions (couplings)  $b_{ij}$  between them are represented by lines [the  $b_{ij}(t)$  are depicted by solid lines, and the  $b_{ij}(0)$  by

dashed lines]. For example,

$$R(t) = \frac{4}{N} \sum \langle \overline{|i, jkl|_t} \overline{|i, jkl|_0} \rangle = \text{[diagram]} + 3 \text{[diagram]}$$

$$= N^{-1} \sum \{ (b_{ij}(t)b_{ik}(t)b_{il}(t)b_{ij}(0)b_{ik}(0)b_{il}(0)) + 3 (b_{ij}(t)b_{ik}(t)b_{il}(t)b_{ji}(0)b_{jk}(0)b_{ji}(0)) \}. \quad (3.5)$$

For the remaining correlation functions we confine ourselves to the graphical expressions, since their explicit forms are easily written out according to the rules indicated:

$$F(t) = \frac{2}{N} \sum \langle \overline{|i, jkl|_t} \rangle = \text{[diagram]} + \text{[diagram]}$$

$$L(t) = \frac{12}{N} \sum \langle \overline{(i, jkl)_t} \overline{(i, jkl)_0} \rangle$$

$$= \text{[diagram]} + 2 \text{[diagram]} + \text{[diagram]} + 2 \text{[diagram]} + 4 \text{[diagram]} + \text{[diagram]} + \text{[diagram]},$$

$$P(t) = \frac{16}{N} \sum \langle \overline{[(jkl) - (kij)]_t} \overline{[(jkl) - (kij)]_0} \rangle = 8 \text{[diagram]}$$

$$+ 8 \text{[diagram]} + 4 \text{[diagram]} - 16 \text{[diagram]} - 16 \text{[diagram]} + 4 \text{[diagram]} + 8 \text{[diagram]},$$

$$A(t) = N^{-1} \sum \langle A_{ij}(t)A_{ij}(0) \rangle = \frac{1}{2} \text{[diagram]} + \frac{1}{2} \text{[diagram]} - \text{[diagram]}$$

$$- \text{[diagram]} - 2 \text{[diagram]} + \text{[diagram]} + \frac{1}{2} \text{[diagram]} + 2 \text{[diagram]} + \frac{1}{2} \text{[diagram]}$$
(3.6)

The functions (2.15) are expressed in terms of the correlation functions (3.5) and (3.6) in the following manner:

$$G_2(t) = G_2^{(2)}(t) + G_2^{(4)}(t),$$

$$G_2^{(2)}(t) = 9 \cdot 2^9 \xi^4 A(t), \quad (3.7)$$

$$G_2^{(4)}(t) = 72 \xi^4 \{ 29R(t) - 24F(t) + 8P(t) + 28L(t) \},$$

$$G_4(t) = 450 \xi^4 \{ 3R(t) + 4L(t) + 24F(t) \}.$$

After the correlation functions (3.5) and (3.6) are found for a specific motion model, Eqs. (3.7), (2.14), and (2.15) make it possible to find the desired contribution  $1/T_{1\rho\rho}^{(4)}$  of the interaction (2.9), which we divide into two parts corresponding to the two-spin and four-spin interactions in  $\mathcal{H}_{\text{eff}}^{(4)}$  (3.2):

$$1/T_{1\rho\rho}^{(4)} = 1/T_{(2)} + 1/T_{(4)}.$$

To analyze the relaxation process we take the two simplest models of the motion of atoms: 1) independent motion; 2) correlated motion. In the former case each atom varies its coordinates independently of the other atoms, while in the latter case the coordinates of all the atoms vary simultaneously. We describe the variation of the positions of the atoms by a Markovian random process with correlation time  $\tau_c$ , for which we represent the correlation functions (3.5) and (3.6) in the form

$$R(t) = R(0) \exp(-|t|/\tau_c), \quad L(t) = L(0) \exp(-|t|/\tau_c),$$

$$P(t) = P(0) \exp(-|t|/\tau_c), \quad F(t) = F(0) \exp(-|t|/\tau_c),$$

$$A(t) = A(0) \exp(-|t|/\tau_c). \quad (3.8)$$

In model (2) we have  $r=l=p=f=a=1$ . In model (1) we take  $r=l=p=f=4$  and  $a=2$  for the calculations. In fact, for the correlation function  $A(t)$  the displacements of atoms  $i$  and  $j$  and of atoms  $k$  are inequivalent. When the latter move over a lattice with equivalent sites, the sum in the definition of the  $A_{ij}$  remains unchanged.

When the foregoing statements are taken into account and (3.8) has been substituted into (3.7), from (2.14) and (2.15) we obtain

$$1/T_{(2)} = 2^{-2} \cdot 9^{-2} M_{2d} \varepsilon^4 A g_2(2\omega_3), \quad (3.9)$$

$$1/T_{(4)} = 2^{-8} \cdot 9^{-2} M_{2d} \varepsilon^4 \{25V_4 g_4(4\omega_3) + V_2 g_4(2\omega_3)\}, \quad (3.10)$$

where

$$A = A(0)/B^3, \quad B = N^{-1} \sum b_{ij}^2 = 4M_{2d}/9,$$

$$V_2 \{29R(0) + 28L(0) + 8P(0) - 24F(0)\}/B^3,$$

$$V_4 = \{3R(0) + 4L(0) + 24F(0)\}/B^3,$$

$$g_n(\omega) = \tau_n / (1 + \omega^2 \tau_n^2) \quad (3.11)$$

is a Lorentzian function with a parameter that depends on the motion model

$$\tau_n = \begin{cases} \tau_c / n - \text{independent motion,} \\ \tau_c - \text{correlated motion.} \end{cases}$$

The coefficients in (3.10) are expressed in terms of lattice sums, whose structure is clear from the diagrams (3.5) and (3.6). These sums were calculated for a simple cubic lattice in Refs. 18–20 and three orientations of the magnetic field relative to the crystallographic axes (to match the accuracy the sums from Ref. 18 were recalculated for a large number of lattice sites). The calculated values of the coefficients are presented in Table I. The last column in Table I contains the values of these coefficients in the limit of an infinite lattice<sup>19,21</sup> keeping only the lattice sums not containing loops of couplings, which have the following structures

TABLE I. Coefficients in the equations for  $T_{\rho\rho\rho}^{(4)}$ .

	[100]	[110]	[111]	$d=\infty$
A	0.51	0.36	0.52	1
$V_2$	100	124	132	121
$V_4$	7.0	11.6	11.9	7



When we calculated  $\mathcal{H}_{\text{eff}}^{(4)}$  above from the second-order equation (2.9), we omitted the contribution from the variation of the rf field in (2.6), since it leads to corrections of the next order. A contribution of comparable magnitude is obtained in first order after (2.6) is substituted into (2.8). It takes into account the spread of the magnitude of the secular part of the dipolar interaction in (2.5) over the sample because of the orientation of the effective field differs from the average. This correction has an operator part, as in the case of  $\mathcal{H}_{ee1}^{+2}$  in (3.2); therefore, it results in a change in  $A_{ij}$  amounting to

$$A'_{ij} = A_{ij} - \frac{8}{3} \omega_e^2 \eta_i b_{ij}, \quad (3.12)$$

and a change in the correlation function  $A(t)$  amounting to

$$A'(t) = A(t) + \frac{64}{9} \omega_e^4 \eta^2 B(t), \quad (3.13)$$

where  $B(t) = N^{-1} \sum \langle b_{ij}(t) b_{ij}(0) \rangle$  and  $\eta^2 = N^{-1} \sum \times (H_{1i} - \langle H_1 \rangle)^2 / \langle H_1 \rangle^2$  is the mean square of the relative nonuniformity of the rf field. In deriving (3.13) we took into account that the averaging with respect to the motion and the averaging with respect to the nonuniformity of the rf field are carried out independently and that  $\langle \eta_i \rangle = 0$ .

#### 4. CONTRIBUTION OF THE EFFECTIVE HAMILTONIAN $\mathcal{H}_{\text{eff}}^{(5)}$ INDUCED BY THE SECOND FIELD TO THE SPIN-LATTICE RELAXATION

Substituting (2.12) into (2.8) and calculating the commutators, we find

$$\begin{aligned} \mathcal{H}_{\text{eff}}^{(5)} = & -\omega_2^{-1} \xi^2 \sum C_{11}(i) I_i^z - 2\omega_2^{-1} \xi^2 \sum \left( I_i^z I_k^- I_j^+ \{ \overline{jk}, i \} + I_i^z I_j^z I_k^z \{ ijk \} \right) \\ & - 2\omega_2^{-1} \xi^2 \sum \left( I_q^+ I_i^+ I_j^- I_k^- I_i^z \{ \overline{ql}, \overline{jk}, i \} - I_i^z I_j^z I_i^z I_k^- I_q^+ \{ ijl, \overline{kq} \} \right. \\ & \left. + I_i^z I_j^z I_k^z I_q^z \{ ijkql \} \right), \end{aligned} \quad (4.1)$$

where we have introduced the following compact notation for the coefficients:

$$\begin{aligned}
C_{11}(i) &= \sum_{j,k} (3\beta_{ijk}^2 + 2\alpha_{k,ij}^2 - \alpha_{i,kj}^2 + \zeta_{i,kj}^2/4) + 2\Delta_i^2, \\
[ijk] &= 2\beta_{ijk}^2 - 2\alpha_{k,ij}^2 + 2\zeta_{k,ij}\Delta_k + \sum_l \zeta_{k,lj}\zeta_{k,il}, \\
\{jk,i\} &= \sum_l (6\beta_{il}\beta_{ilj} + 2\alpha_{k,il}\alpha_{j,il} + 2\alpha_{l,ij}\alpha_{l,ik} \\
&\quad - 2\alpha_{i,lj}\alpha_{i,lk} - \zeta_{k,il}\zeta_{j,lk} - 2\alpha_{k,jl}\zeta_{l,ji} + 2\alpha_{k,lj}\zeta_{l,ki}) \\
&\quad + 4\Delta_i\alpha_{k,ij} - 2\Delta_j\zeta_{k,ji}, \quad (4.2) \\
\{ql,jk,i\} &= 3\beta_{ijk}\beta_{iql} - \alpha_{i,ql}\alpha_{i,kj} + 4\alpha_{k,il}\alpha_{q,ij} \\
&\quad - 4\alpha_{j,ql}\zeta_{k,qi} + 2\alpha_{j,lq}\zeta_{k,ij}, \\
[ijl,kq] &= 2\zeta_{k,ij}\zeta_{q,kl} - 4\alpha_{k,ql}\zeta_{l,ij}, \\
\{ijkql\} &= \zeta_{k,ij}\zeta_{k,ql}.
\end{aligned}$$

According to (4.2), the three-spin interaction in (4.1) consists of a correction due to the doubly averaged dipolar interaction and a correction due to the variation of the strength of the effective field over the sample, primarily because of the non-uniformity of the rf field. The presence of the detuning  $\Delta_i$  makes the second effective field deviate from its "magic" orientation  $\theta' = \pi/2$  and consequently leads to incomplete averaging of the first-order effective Hamiltonian  $\mathcal{H}_{\text{eff}}^{(3)}$ .

In (4.1) the  $z$  axis is parallel to the second field. To calculate the spin-lattice relaxation of the magnetization parallel to the third field, we move over to a new reference frame with the  $z$  axis of that field perpendicular to the second field, and we divide the Hamiltonian into the nonsecular parts  $\mathcal{H}_{ee}^m$  ( $m = \pm 1, \pm 3, \pm 5$ ), which satisfy the condition (2.4) for the third field. Each such part, in turn, consists of the terms  $\mathcal{H}_{ee}^m(p)$ , which differ with respect to the form of the operator expressions  $\hat{O}_{mp}(ijkql)$ ,

$$\mathcal{H}_{ee}^m(p) = -\frac{\xi^2}{\omega_2} \sum C_{mp}(ijkql) \hat{O}_{mp}(ijkql),$$

where the summation is performed over the lattice indices (one, three, or five) present in the respective part. The index  $p$  labels the different contributions for an assigned  $m$ , whose sum gives  $\mathcal{H}_{ee}^m$ . The results obtained for the operator expressions and the coefficients in front of them are presented in Table II.

After  $\mathcal{H}_{ee}^m$  has been substituted into (2.15) and the traces of the matrices have been calculated, we obtain

$$\begin{aligned}
G_1(t) &= 2^{-1}C_{11}(t) + 2^{-2}C_{12}(t) + 2^{-4}C_{13}(t) \\
&\quad + 3 \cdot 2^{-2}C_{14}(t) + 2^{-7}C_{15}(t) + 3 \cdot 2^{-9}C_{16}(t), \\
G_3(t) &= 3 \cdot 2^{-4}C_{31}(t) + 3 \cdot 2^{-7}C_{32}(t) + 3 \cdot 2^{-8}C_{33}(t), \\
G_5(t) &= 15 \cdot 2^{-8}C_5(t),
\end{aligned} \quad (4.3)$$

where

$$C_{mp}(t) = \xi^4 N^{-1} \sum \langle C_{mp}(ijkql;t) C_{mp}(ijkql;0) \rangle \quad (4.4)$$

is the correlation function of the coefficients listed in the fourth column of Table II with summation over five, three, or one lattice index, depending on the coefficient. On the basis of Table II, Eqs. (4.2) and (2.13), and the symmetrization rules, we can calculate the correlation functions (4.4) for an assigned motion (at least numerically) and then find the corresponding contribution to  $1/T_{1\rho\rho\rho}$ , which we write in the form

$$1/T_{1\rho\rho\rho}^{(5)} = 1/T_{(1)} + 1/T_{(3)} + 1/T_{(5)},$$

separating the contributions from the one-, three-, and five-spin interactions to  $\mathcal{H}_{\text{eff}}^{(5)}$ . The expressions for the coefficients  $C_{mp}(ijkql)$  directly in terms of products of the dipolar coupling constants  $b_{ij}$  are given in the Appendix.

Let us consider the same two motion models as in the preceding section, for which

$$C_{mp}(t) = C_{mp}(0) \exp\{-|t|f_{mp}/\tau_c\}. \quad (4.5)$$

The coefficient  $f_{mp}$  in the exponent is equal to unity in the case of correlated motion and to the number of summation indices in (4.4) in the case of independent motion. Since the spins move between equivalent sites in the system under consideration, the contribution of the dipolar interaction to  $C_{11}(t)$  will not vary with time, and the coefficients  $\{jk,i\}$  and  $[ijk]$  defined in (4.2) will not vary with the position of the atom having index  $l$ , over which the summation over all the sites is performed. Moreover, the temporal variation of the contribution due to nonuniformity of the rf field can be neglected in  $C_{11}(t)$ . In fact, it is a macroscopic quantity, while the motion is microscopic. The mean part of  $\Delta_i$  does not make a contribution to the longitudinal relaxation, and it is understood to be included in  $\omega_e$ . Therefore, the pre-exponential factor  $C_{11}(0)$  in (4.5) vanishes.

The remaining pre-exponential factors in (4.5) are calculated in the Appendix in the approximation of lattices of large dimensionality. [As we saw in the preceding section in the example of lattice sums with four summation indices for a simple cubic lattice (Table I), this approximation faithfully conveys the relationship between the different contributions to the relaxation rate.] After substituting (4.5) into (4.3) and then into (2.14), we obtain

$$\begin{aligned}
1/T_{(3)} &= M_2(3;1)g_3(3\omega_3) + [M_2(1;2) \\
&\quad + M_2(1;3)]g_3(\omega_3), \\
1/T_{(5)} &= M_2(5)g_5(5\omega_3) + [M_2(3;2) \\
&\quad + M_2(3;3)]g_5(3\omega_3) + [M_2(1;4) + M_2(1;5) \\
&\quad + M_2(1;6)]g_5(\omega_3),
\end{aligned} \quad (4.6)$$

where the function  $g_n(\omega)$  is defined in (3.11) and the  $M_2(m,n)$  are the contributions of the corresponding parts of the effective interaction to the second moment  $M_{2\rho\rho}$ . The values of these contributions in the  $d = \infty$  approximation are presented in the last column of Table II.

TABLE II. Operator expressions and coefficients for the parts  $\mathcal{H}_{\text{eff}}^m(p)$  of the effective Hamiltonian  $\mathcal{H}_{\text{eff}}^{(5)}$  that are nonsecular in the third field and their corresponding contributions to  $M_{2\rho\rho}$ .

$m$	$p$	$\hat{O}_{mp}(ijkl)$	$C_{mp}(ijkl)$	$M_2(mp)\omega_2^2(32\omega_e)^4 B^{-4}$
1	1	$I_i^+ / 2$	$C_{11}(i)$	18496
1	2	$I_i^+ I_j^+ I_k^+$	$\overline{\{jk, i\}}$	$2^5 \cdot 3553 / 9 + \eta^2 \cdot 44 \cdot (8\omega_e)^4 B^{-2}$
1	3	$\frac{I_i^- I_j^+ I_k^+}{4}$	$3\overline{\{ijk\}} + 3\overline{\{ik, j\}} - 2\overline{\{jk, i\}}$	$2^3 \cdot 675 + \eta^2 \cdot 11 \cdot (8\omega_e)^4 B^{-2}$
1	4	$I_q^+ I_i^+ I_j^+ I_k^+ I_l^+$	$\overline{\{ql, jk, i\}}$	198827/18
1	5	$\frac{I_q^+ I_i^+ I_j^+ I_k^+ I_l^-}{4}$	$6\overline{\{ql, jk, i\}} - 4\overline{\{ql, jk, i\}} + 8\overline{\{qj, lk, i\}} - 12\overline{\{qj, lk, i\}} + 3\overline{\{ijk, lq\}}$	814407/(9 · 4)
1	6	$\frac{I_i^- I_k^- I_j^+ I_q^+ I_l^+}{16}$	$10\overline{\{ql, ki, j\}} - 8\overline{\{ql, jk, i\}} + 10\overline{\{ikjql\}} - 10\overline{\{ijl, kl\}} + 2\overline{\{jlq, ik\}} + 6\overline{\{ikj, ql\}}$	1390063/(9 · 16)
3	1	$\frac{I_i^+ I_j^+ I_k^+}{4}$	$\overline{\{jk, i\}} - \overline{\{ijk\}}$	$2^3 \cdot 8281 + \eta^2 \cdot 21^2 \cdot (8\omega_e)^4 B^{-2}$
3	2	$\frac{I_q^+ I_j^+ I_i^+ I_l^+ I_k^+}{4}$	$4\overline{\{ql, jk, i\}} - 2\overline{\{qj, lk, i\}} + \overline{\{ikl, jq\}}$	400477/4
3	3	$\frac{I_i^- I_j^+ I_k^+ I_q^+ I_l^+}{16}$	$2\overline{\{ql, jk, i\}} - 5\overline{\{ql, jk, i\}} + 5\overline{\{ijl, kq\}} - 4\overline{\{kjl, iq\}} + 5\overline{\{ijkql\}}$	2694559/32
5		$\frac{I_i^+ I_j^+ I_k^+ I_q^+ I_l^+}{16}$	$\overline{\{ql, jk, i\}} + \overline{\{ijl, kq\}} + \overline{\{ijkql\}}$	16506875/(9 · 32)

## 5. DISCUSSION

The expressions (3.9), (3.10), and (4.6) describe the spin-lattice relaxation of the magnetization parallel to the third field in a triply rotating reference frame for ultraslow motions with correlation frequencies  $\tau_c^{-1} \sim \omega_3 \ll \omega_2$ . According to the theory of averaging, when there are random motions<sup>7,17</sup> with  $\tau_c^{-1} \sim \omega_2$ , the mean Hamiltonian for the second field  $\mathcal{H}_{\text{eff}}^{(5)}$  does not form, and relaxation takes place in the doubly rotating frame, being caused directly by the effective Hamiltonian  $\mathcal{H}_{\text{eff}}^{(3)}$ , which varies rapidly with time under the action of the motions and the field  $\omega_2$ . For the contribution to the relaxation rate of the magnetization that is orthogonal to the second field from the parts of the effective Hamiltonian that are nonsecular in the second field, we find

$$\begin{aligned} \frac{1}{T_{2\rho\rho}'} &= \frac{3}{2^{10}\omega_e^2 N} \sum \{127J_{ijk,ijk}(\omega_2) + 206J_{ijk,jik}(\omega_2)\} \\ &+ \frac{147}{2^{10}\omega_e^2 N} \sum \{J_{ijk,ijk}(3\omega_2) + 2J_{ijk,jik}(3\omega_2)\} \\ &+ \frac{9}{2^7\omega_e^2 N} \sum J_i(\omega_2), \end{aligned} \quad (5.1)$$

where  $J_{ijk,pql}(\omega)$  and  $J_i(\omega)$  are the Fourier transforms of the correlation functions  $\langle b_{ij}(t)b_{ik}(t)b_{pq}(0)b_{pl}(0) \rangle$  and  $\langle \sum_j b_{ij}^2(t) \sum_q b_{iq}^2(0) \rangle$ , respectively. The same correlation functions, but preceded by different coefficients, appear in the expression for  $T_{1\rho\rho}$  (Ref. 6). The presence of the weak third field parallel to the magnetization has scarcely any influence on the size of the contribution (5.1). At the same time, the contribution to the relaxation from the parts of the effective Hamiltonian that are secular in the second field is influenced by the third field, as is reflected in the equations for  $T_{1\rho\rho\rho}$ .

In addition, when  $\tau_c^{-1} \sim \omega_2$ , the relaxation rate varies under the action of the second-order effective Hamiltonian  $\mathcal{H}_{\text{eff}}^{(4)}$  because of the additional contribution from the parts that are nonsecular in  $\omega_2$ . We shall not take them into account in view of the smallness of the contribution from the second-order terms in this range of motions.

When the intensity of the motions increases further ( $\tau_c^{-1} \sim \omega_e$ ), an effective Hamiltonian does not develop,<sup>7,17</sup> and the relaxation is governed by the dipolar interaction (2.6), which varies with time under the action of the rf field and the thermal motions. When the rotation of the magneti-



zation about the second field is taken into account, for the relaxation rate we obtain

$$\frac{1}{T_{1e}} = \frac{1}{2} \left( \frac{1}{T_{2\rho}} + \frac{1}{T_{1\rho}} \right), \quad (5.2)$$

where  $\tau_{1\rho}$  and  $\tau_{2\rho}$  are the well known<sup>1,2,6,7</sup> longitudinal and transverse relaxation times in a rotating frame.

The relaxation mechanisms (5.1) and (5.2) operate when there are ultraslow motions, although they are less dominant than the contributions considered in the preceding sections. When they are taken into account, for the spin-lattice relaxation rate in the triply rotating frame we obtain

$$\frac{1}{T_{1\rho\rho\rho}} = \frac{1}{T_{1e}} + \frac{1}{T'_{2\rho\rho}} + \frac{1}{T_{(2)}} + \frac{1}{T_{(3)}} + \frac{1}{T_{(4)}} + \frac{1}{T_{(5)}}. \quad (5.3)$$

As the intensity of the atomic and molecular motions increases, the last four terms should be eliminated first from (5.3), and then  $1/T'_{2\rho\rho}$  should be removed. However, we shall use Eq. (5.3) in the calculations over the entire range, since in the region of fast motion these contributions are so small that retaining them has practically no effect on the result.

The full expression (5.3) is composed of contributions from correlation functions with different numbers of atoms (spins). The separation of these contributions can be greatly furthered by studying the dependence of  $T_{1\rho\rho\rho}$  on the parameters of the rf field. Besides the parameters already introduced in (5.3), the orientations of the fields can also be varied. When the angles  $\theta$  and  $\theta'$  deviate from their magic values, new terms, which cause an abrupt increase in  $1/T_{1\rho\rho\rho}$ , appear in the effective Hamiltonian.<sup>12-14</sup> The slow dependence of the terms already taken into account on  $\theta$  and  $\theta'$  can be neglected on their background. In this approximation the spin-lattice relaxation can be described by the former equations, in which the coefficients (A5), (A6), and (3.12) should be altered by including the contributions from the following new terms in them:

$$A_{ij}(\theta) = A'_{ij} + 2\omega_e^2(3\cos^2\theta - 1)b_{ij},$$

$$D(\theta') = D - \frac{3\cos\theta'}{4\omega_e},$$

$$E(\theta') = E + \frac{9\cos\theta'}{8\omega_e},$$

$$Q(\theta') = Q + \frac{3\cos\theta'}{8\omega_e}.$$

When everything stated above is taken into account, we obtain the following final expressions for the different contributions to Eq. (5.3) for the spin-lattice relaxation time:

$$\frac{1}{T_{1e}} = \frac{M_{2d}}{18} \{7g_2(\omega_e) + 5g_2(2\omega_e)\},$$

$$\frac{1}{T'_{2\rho\rho}} = \frac{M_{2d}}{12^3} \varepsilon^2 \{49g_3(3\omega_2) + 127g_3(\omega_2)\},$$

$$\frac{1}{T_{(2)}} = 1.58 \cdot 8^{-3} M_{2d} g_2(2\omega_3) \{[\varepsilon^2 - 4.5(3\cos^2\theta - 1)]^2 + 36\eta^2\},$$

$$\frac{1}{T_{(3)}} = 8^{-3} M_{2d} g_3(3\omega_3) [1.26\varepsilon^2(\varepsilon K_2 + 12.5\cos\theta')^2 + 87.1K_2^2\eta^2] + 8^{-3} M_{2d} g_3(\omega_3) \{0.344\varepsilon^4 K_2^2 + 4.80\varepsilon^3 K_2 \cos\theta' + 24.4\varepsilon^2 \cos^2\theta' + 10.9K_2^2\eta^2\},$$

$$\frac{1}{T_{(4)}} = 8^{-3} M_{2d} \varepsilon^4 \{4.32g_4(4\omega_3) + 2.99g_4(2\omega_3)\},$$

$$\frac{1}{T_{(5)}} = 8^{-3} M_{2d} \varepsilon^4 K_2^2 \{1.09g_5(5\omega_3) + 3.51g_5(3\omega_3) + 0.83g_5(\omega_3)\}, \quad (5.4)$$

where we have written  $K_2^2 = M_{2d}/\omega_2^2$  and the remaining parameters have already been defined above.

To select the values of the parameters in Eqs. (5.4), we take solid benzene, CaF<sub>2</sub>, and PbF<sub>2</sub>. Reorientation of the molecules in benzene can be regarded as an example of correlated motion,<sup>7,21,22</sup> while diffusion in CaF<sub>2</sub> and PbF<sub>2</sub> (Ref. 23) can be regarded as an example of independent motions. Taking published values of the second moments  $M_{2d}$  of the NMR absorption line and the effective frequency  $\omega_e/2\pi = 100$  kHz used in experiments,<sup>11-16</sup> we obtain the following values of  $\varepsilon$ : in benzene, 0.125 for stationary molecules and 0.051 for rapidly rotating molecules; in CaF<sub>2</sub>, 0.06 in the [111] orientation and 0.144 in the [100] orientation; in PbF<sub>2</sub>, 0.048 and 0.115 in the same orientations, respectively.

The choice of the field strengths  $\omega_2$  and  $\omega_3$  in Eqs. (5.4) is not entirely arbitrary, since a field strength  $\omega_2 \gg M_{2\rho}^{1/2} \approx 0.45\varepsilon M_{2d}^{1/2}$  must be achieved to effect secondary averaging. In turn, the conditions for spin locking in the third field require  $\omega_3$  to exceed the mean local field in the doubly rotating reference frame. Since the mean square of the local field is significantly smaller than the second moment in the doubly rotating frame  $M_{2\rho\rho}$ , it is more convenient for us to take the value of  $M_{2\rho\rho}^{1/2}$  as the lower bound for  $\omega_3$ . We obtain an estimate for  $M_{2\rho\rho}$  in the approximation under consideration by assembling the coefficients in (5.4):

$$M_{2\rho\rho} = M_{2\rho\rho}^{(2)} + M_{2\rho\rho}^{(3)} + M_{2\rho\rho}^{(4)} + M_{2\rho\rho}^{(5)}, \quad (5.5)$$

where  $M_{2\rho\rho}^{(n)}$  is the contribution from the  $n$ -spin effective interaction:

$$\begin{aligned} M_{2\rho\rho}^{(2)} &= 1.58 \cdot 8^{-3} M_{2d} \{[\varepsilon^2 - 4.5(3\cos^2\theta - 1)]^2 + 36\eta^2\}, \\ M_{2\rho\rho}^{(3)} &= 8^{-3} M_{2d} \{1.61\varepsilon^4 K_2^2 + 36.3\varepsilon^3 k_2 \cos\theta' + 220.4\varepsilon^2 \cos^2\theta' + 98.0K_2^2\eta^2\}, \end{aligned} \quad (5.6)$$

$$M_{2\rho\rho}^{(4)} = 7.31 \cdot 8^{-3} M_{2d} \varepsilon^4,$$

$$M_{2\rho\rho}^{(5)} = 5.43 \cdot 8^{-3} M_{2d} \varepsilon^4 K_2^2.$$

The dependence of  $T_{1\rho\rho\rho}$  on  $\tau_c$  was calculated from Eqs. (5.3) and (5.4) for various values of the parameters of the rf field. Several characteristic curves are shown in the figures. To simplify the analysis, all the frequencies are assigned in

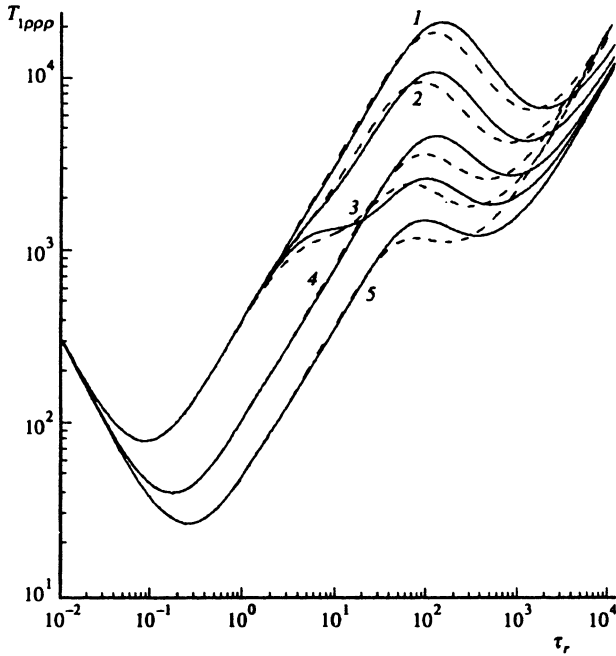


FIG. 1. Plots of the dependence of  $T_{1\rho\rho\rho}$  on  $\tau_r$  for independent (solid lines) and correlated (dashed line) motions for magic-angle-spinning conditions,  $\eta = 1 \times 10^{-3}$ , and various values of the fields: 1)  $\omega_e = 20$ ,  $\omega_2 = 1$ ,  $\omega_3 = 0.72 \times 10^{-3}$ ; 2)  $\omega_e = 20$ ,  $\omega_2 = 0.5$ ,  $\omega_3 = 1.16 \times 10^{-3}$ ; 3)  $\omega_e = 20$ ,  $\omega_2 = 0.2$ ,  $\omega_3 = 2.68 \times 10^{-3}$ ; 4)  $\omega_e = 10$ ,  $\omega_2 = 1$ ,  $\omega_3 = 1.86 \times 10^{-3}$ ; 5)  $\omega_e = 20/3$ ,  $\omega_2 = 1$ ,  $\omega_3 = 4.02 \times 10^{-3}$ .

units of  $M_{2d}^{1/2}$  (the times are given in units of  $M_{2d}^{-1/2}$ ), and  $\tau_r$ , which is equal to  $\tau_c$  for independent motions and  $2\tau_c$  for correlated motions. With this a choice we achieve juxtaposition of the curves in the region of the principal minimum at  $\tau_r = 2/\omega_e$  from  $1/T_{1e}$  in (5.3) expressed in terms of two-particle correlation functions. Besides the principal minimum, the curves in Fig. 1 exhibit a step at  $\tau_r = 2/\omega_e$  from  $1/T_{2\rho\rho}$  and, finally, a minimum or a step at  $\tau_r \sim 1/\omega_3$ . Since the latter minimum becomes deeper as  $\omega_3$  decreases (compare the upper curves in Figs. 1 and 2), the curves in Fig. 1 were constructed for  $\omega_3 = M_{2\rho\rho}^{1/2}$ . In the slow-motion limit  $\tau_r \rightarrow \infty$  the curves approach the asymptotic dependence

$$1/T_{1\rho\rho\rho} \sim M'_{2\rho\rho} / \omega_3^2 \tau_r, \quad (5.7)$$

which corresponds to straight lines in the figures. The coefficient  $M'_{2\rho\rho}$  differs from  $M_{2\rho\rho}$  in that the coefficient in front of  $g_n(p\omega_3)$  in (5.4) appears with the multiplier  $p^{-2}$  for correlated motions and with  $n/2p^2$  for independent motions. Since  $M'_{2\rho\rho} \sim M_{2\rho\rho}$  holds, these curves follow asymptotic behavior (5.7) with a coefficient close to unity at the values of  $\omega_3 = M_{2\rho\rho}^{1/2}$  selected for the curves in Fig. 1. At the same time, the right-hand limb of the principal minimum has the dependence

$$1/T_{1\rho\rho\rho} \approx 1/T_{1e} \sim \varepsilon^2 / \tau_r.$$

Thus, the corresponding parts of the curves have the form of two segments of the indicated straight lines joined by a segment with the inverse dependence

$$1/T_{1\rho\rho\rho} \sim \sum_n M_{2\rho\rho}^{(n)} \tau_n. \quad (5.8)$$

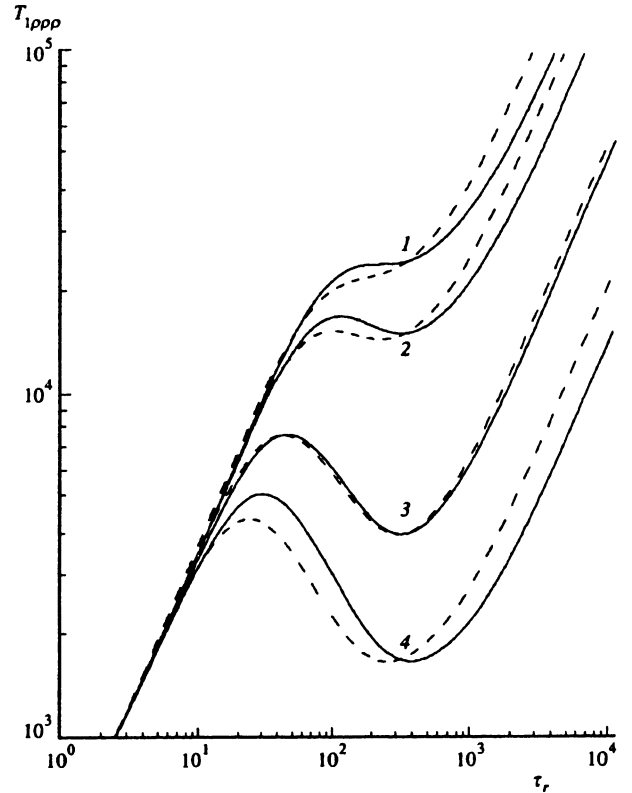


FIG. 2. Plots of the dependence of  $T_{1\rho\rho\rho}$  on  $\tau_r$  in the slow-motion region (solid lines – independent motions; dashed lines – correlated motions) in systems with a weak dipolar interaction for  $\varepsilon = 0.05$ ,  $\omega_2 = 1$ ,  $\omega_3 = 3.14 \times 10^{-3}$ , and the following values of the remaining parameters: 1)  $\theta = \theta_M$ ,  $\theta' = 90^\circ$ ,  $\eta = 1 \times 10^{-3}$ ; 2)  $\theta = \theta_M$ ,  $\theta' = 90^\circ$ ,  $\eta = 1.5 \times 10^{-3}$ ; 3)  $\theta = 54.6^\circ$ ,  $\theta' = 90^\circ$ ,  $\eta = 1.5 \times 10^{-3}$ ; 4)  $\theta = \theta_M$ ,  $\theta' = 85^\circ$ ,  $\eta = 1.5 \times 10^{-3}$ .

Hence it follows, first, that the distance between these straight lines increases and the minimum at  $\tau_r \sim 1/\omega_3$  deepens as  $\varepsilon$  decreases. Conversely, as  $\varepsilon$  increases, the straight lines approach, and the minimum degenerates into a step. Second, as the remaining parameters of the rf field vary, the portion of the plot of (5.8) between the straight lines (the left-hand wing of the minimum or the step) moves upward or downward, following the variation of  $M_{2\rho\rho}$  (see Fig. 3).

Figure 1 shows that  $T_{1\rho\rho\rho}$  is most sensitive to the motion model in the region  $\tau_r \gtrsim 1/\omega_3$ , while in the region of the principal minimum at  $\tau_r \omega_e = 2$  the curves for the two motion models merge under the definition of  $\tau_r$  chosen in the equations. Figures 2 and 3 show plots of the dependence of  $T_{1\rho\rho\rho}$  on  $\tau_r$  in the slow-motion region for various values of the parameters. Not only the depth of the corresponding minimum and its position, but also the roles of the different terms in (5.4) in the relaxation process vary with the parameters. For example, when we take  $\varepsilon = 0.05$  and the angles have the magic values, i.e., when there is strong narrowing, the main contribution is made by the terms in  $1/T_{(2)}$  and  $1/T_{(3)}$  induced by the nonuniformity of the rf field. As  $\eta$  varies from  $1 \times 10^{-3}$  to  $1.5 \times 10^{-3}$ , a shift corresponding to a 1.6-fold decrease in  $T_{1\rho\rho\rho}$ , which is close to a 2.25-fold increase in  $\eta^2$ , occurs on the upper curves in Fig. 2.

When  $\theta$  deviates from the magic value  $\theta = \theta_M = 54.74^\circ$ , there is a rapid increase in the contribution of  $1/T_{(2)}$  in (5.4), which is expressed, like  $1/T_{2e}$ , in terms of two-particle correlation functions and is, therefore, insensi-

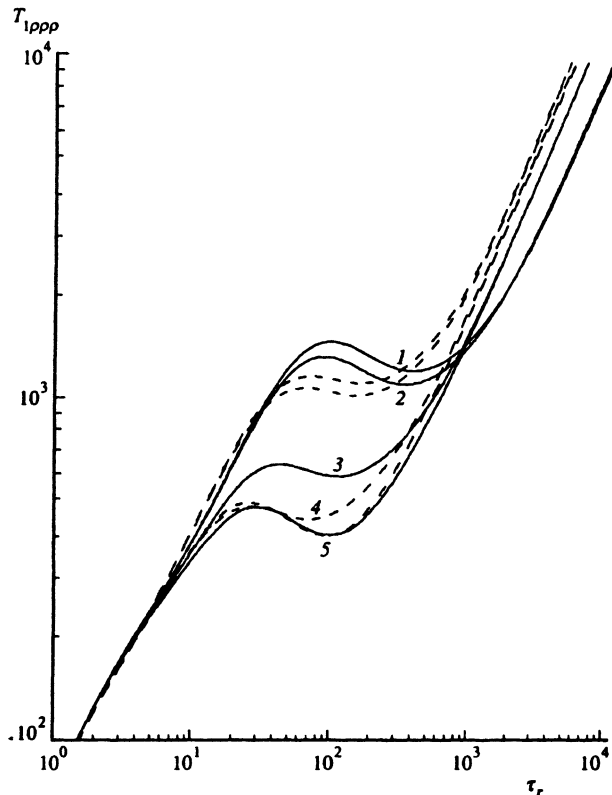


FIG. 3. Plots of the dependence of  $T_{1\rho\rho\rho}$  on  $\tau_r$  in the slow-motional region (solid lines – independent motions; dashed lines – correlated motions) in systems with a strong dipolar interaction for  $\varepsilon=0.125$ ,  $\omega_2=0.5$ ,  $\eta=1.5 \times 10^{-3}$ , and the following values of the remaining parameters: 1)  $\theta=\theta_M$ ,  $\theta'=91.2^\circ$ ,  $\omega_3=4.11 \times 10^{-3}$ ; 2)  $\theta=\theta_M$ ,  $\theta'=90^\circ$ ,  $\omega_3=4.44 \times 10^{-3}$ ; 3)  $\theta=\theta_M$ ,  $\theta'=86^\circ$ ,  $\omega_3=9.32 \times 10^{-3}$ ; 4)  $\theta=\theta_M$ ,  $\theta'=85^\circ$ ,  $\omega_3=9.32 \times 10^{-3}$ ; 5)  $\theta=54^\circ$ ,  $\theta'=90^\circ$ ,  $\omega_3=M_{2\rho\rho}^{1/2}=9.32 \times 10^{-3}$ .

tive to the motion model (under the definition of  $\tau_r$  chosen). This property is clearly seen from the corresponding curves in Figs. 2 and 3.

When the deviation of  $\theta'$  from the magic value of  $90^\circ$  is sufficiently great, the contribution of  $1/T_{(3)}$ , which is expressed in terms of three-spin correlation functions that have a dependence on the motion model different from that of the two-particle functions, increases. Consequently, the minima on the curves for  $\theta'=85^\circ$  in Fig. 2 for correlated and independent motions move in opposite directions away from the minimum of the curve for  $\theta=54.6^\circ$ . This property of the curves enables us, in principle, to draw a qualitative conclusion regarding the motion model from the positions of the minima on the corresponding experimental plots of the temperature dependence.

Conversely, when the deviation of  $\theta'$  from  $90^\circ$  is small, the contribution of  $1/T_{(3)}$  can decrease, as is demonstrated by the upper curve in Fig. 3. The value  $\theta'=91.2^\circ$  was taken for it, since under the conditions selected the contribution of  $M_{2\rho\rho}^{(3)}$  reaches its minimum value at this value of the angle.

The degree of narrowing of the line decreases ( $\varepsilon$  increases) in substances with a large value of  $M_{2d}$ . In such cases, as is seen in Fig. 1 and Fig. 3, the minimum becomes indistinct and resembles a step. Motion can also be studied on the basis of such curves. In addition, as  $\varepsilon$  increases, the sensitivity to the motion model increases due to the increase in the contributions of  $1/T_{(4)}$  and  $1/T_{(5)}$ , which are ex-

pressed in terms of four- and five-particle correlation functions. For example, while the ratio between the values of  $1/T_{(3)}$  for correlated and independent motion equals 1.5 in the limit  $\tau_r \rightarrow \infty$ , the ratios for  $1/T_{(4)}$  and  $1/T_{(5)}$  are equal to 2 and 2.5. On the calculated curves with the magic values of  $\theta$  and  $\theta'$  this ratio equals 1.4 at  $\tau_r=10^4$  in the case of  $\varepsilon=0.05$  (Fig. 2). At  $\varepsilon=0.125$  (Fig. 3), it equals 2.01, and at  $\theta'=91.2^\circ$ , it even increases to 2.11 because of the decrease in the contribution of  $1/T_{(3)}$ . As in the preceding case of Fig. 2, qualitative conclusions regarding the motion model can be drawn in Fig. 3 by comparing the curves for  $\theta \neq \theta_M$  and  $\theta' \neq 90^\circ$ , although the comparison procedure changes. For this purpose we plotted a curve for  $\theta=54^\circ$  and  $\omega_3=M_{2\rho\rho}^{1/2}$  in Fig. 3. Then the values of  $\theta'$  were determined separately for correlated and independent motions from the condition that the values of  $T_{1\rho\rho\rho}$  coincide at  $\tau_r=10^4$ . Good agreement was obtained (as is seen in Fig. 3) for  $\theta'=85^\circ$  and  $\theta'=86^\circ$ . The curves diverge as  $\tau_r$  decreases. The curve for independent motions is appreciably higher than the curve for  $\theta=54^\circ$ , and the curve for correlated motions practically coincides with the latter, except in a small neighborhood about the minimum. This behavior of the curves for correlated motion arises because we have  $1/T_{1\rho\rho\rho} \sim 2M_{2\rho\rho}^{(3)}/\omega_3^2\tau_r$  for the three-spin contribution in the limit  $\tau_r \rightarrow \infty$ , and on the edge of the step we have  $1/T_{1\rho\rho\rho} \sim M_{2\rho\rho}^{(3)}\tau_r/2$ . In the case of independent motions we have  $3M_{2\rho\rho}^{(3)}/\omega_3^2\tau_r$  and  $M_{2\rho\rho}^{(3)}\tau_r/3$ , respectively. Therefore, when we achieve coincidence between the right-hand portions of the curves by varying  $M_{2\rho\rho}^{(3)}$ , the steps diverge by a factor of  $(3/2)^2$ . The ratio for the five-spin contribution  $1/T_{(5)}$  would be  $(5/2)^2$  for independent motions, as opposed to 1 for correlated motions. The ratios for the calculated curves are smaller than these values due to the presence of other contributions in Eqs. (5.7) and (5.8). However, these differences are large enough to determine the type of motions by comparing calculated and experimental curves even when there are only rough estimates of the lattice sums and correlation functions.

Above we discussed the qualitative aspect of the dependence of  $T_{1\rho\rho\rho}$  on the parameters of the rf field and the temperature. Quantitative separation of the various contributions to  $T_{1\rho\rho\rho}$  at each temperature can be accomplished by solving the system of equations obtained from (5.3) and (5.4) after plugging in the value of  $T_{1\rho\rho\rho}$  measured for several values of the parameters.

Thus, the foregoing analysis of the theoretical expressions obtained for the spin-lattice relaxation time in a triply rotating reference frame shows that the two-, three-, four-, and five-particle correlation functions can actually be studied on the basis of the temperature dependence of the effect of the rf field when its parameters are varied, and new detailed information regarding atomic and molecular mobility in the sample under investigation can ultimately be extracted.

We thank A. E. Mefed for some useful discussions.

This work was carried out with financial support from the Krasnoyarsk Territorial Science Foundation (Project No. 4F0119).

**APPENDIX A:**

We obtain explicit expressions for the coefficients of  $\mathcal{H}_{ee}^m$ , which are listed briefly in Table II. We introduce symbolic representations of the coefficients (2.13) in the form of triangles of three numbers:

(A1)

$$\beta_{ijk} = \frac{7}{3} \left| \begin{array}{c} i \\ 1 \\ 1 \end{array} \right|_k, \quad \zeta_{k,ij} = 4 \left| \begin{array}{c} i \\ -2 \\ -2 \end{array} \right|_k, \quad \alpha_{k,ij} = \left| \begin{array}{c} i \\ 5 \\ 5 \end{array} \right|_k.$$

The correspondence rules are clear from a comparison with (2.13): the number at vertex  $q$  is equal to the coefficient in front of the terms  $b_{ql}b_{qf}$ . The coefficients (4.2) of  $\mathcal{H}_{\text{eff}}^{(5)}$  have the following diagrammatic representations:

$$\begin{aligned} \{ql, jk, i\} &= \frac{7^2}{3} \left| \begin{array}{c} j \\ 1 \\ 1 \end{array} \right|_k \left| \begin{array}{c} q \\ 1 \\ 1 \end{array} \right|_i - \left| \begin{array}{c} j \\ 5 \\ 5 \end{array} \right|_k \left| \begin{array}{c} q \\ -1 \\ -1 \end{array} \right|_i + 4 \left| \begin{array}{c} l \\ 5 \\ -1 \end{array} \right|_k \left| \begin{array}{c} q \\ 5 \\ -1 \end{array} \right|_i \\ &+ 8 \left| \begin{array}{c} l \\ 5 \\ 5 \end{array} \right|_q \left| \begin{array}{c} k \\ -2 \\ -2 \end{array} \right|_i - 4^2 \left| \begin{array}{c} j \\ -1 \\ 5 \end{array} \right|_l \left| \begin{array}{c} k \\ -2 \\ -2 \end{array} \right|_i, \\ [ijl, kq] &= 2 \cdot 4^2 \left| \begin{array}{c} l \\ -2 \\ -2 \end{array} \right|_i \left| \begin{array}{c} k \\ -2 \\ -2 \end{array} \right|_j - 4^2 \left| \begin{array}{c} k \\ -1 \\ 5 \end{array} \right|_q \left| \begin{array}{c} i \\ 1 \\ -2 \end{array} \right|_j, \\ \langle ijkql \rangle &= 4^2 \left| \begin{array}{c} l \\ -2 \\ -2 \end{array} \right|_q \left| \begin{array}{c} i \\ 1 \\ -2 \end{array} \right|_j, \\ \{jk, i\} &= \sum_l \left( 2 \cdot \frac{7^2}{3} k \left| \begin{array}{c} i \\ 1 \\ 1 \end{array} \right|_l \left| \begin{array}{c} j \\ 1 \\ 1 \end{array} \right|_l + 2k \left| \begin{array}{c} i \\ -1 \\ 5 \end{array} \right|_l \left| \begin{array}{c} j \\ 5 \\ -1 \end{array} \right|_l + 2k \left| \begin{array}{c} i \\ 5 \\ -1 \end{array} \right|_l \left| \begin{array}{c} j \\ -1 \\ 5 \end{array} \right|_l \right. \\ &- 2k \left| \begin{array}{c} i \\ 5 \\ 5 \end{array} \right|_l \left| \begin{array}{c} j \\ -1 \\ 5 \end{array} \right|_l - 4^2 i \left| \begin{array}{c} k \\ -2 \\ -2 \end{array} \right|_l \left| \begin{array}{c} j \\ -2 \\ -2 \end{array} \right|_l - 8k \left| \begin{array}{c} j \\ -1 \\ 5 \end{array} \right|_l \left| \begin{array}{c} i \\ 1 \\ -2 \end{array} \right|_l \\ &\left. + 8j \left| \begin{array}{c} k \\ -1 \\ 5 \end{array} \right|_l \left| \begin{array}{c} i \\ -2 \\ -2 \end{array} \right|_l \right) + 4 \left| \begin{array}{c} k \\ -1 \\ 5 \end{array} \right|_j^* - 8 \left| \begin{array}{c} j^* \\ -2 \\ -2 \end{array} \right|_i, \\ [ijk] &= 2 \cdot \frac{7^2}{9} j \left| \begin{array}{c} i \\ 1 \\ 1 \end{array} \right|_k \left| \begin{array}{c} j \\ 1 \\ 1 \end{array} \right|_k - 2k \left| \begin{array}{c} i \\ -1 \\ 5 \end{array} \right|_j \left| \begin{array}{c} j \\ 5 \\ -1 \end{array} \right|_k \\ &+ \sum_l 4^2 j \left| \begin{array}{c} k \\ -2 \\ -2 \end{array} \right|_l \left| \begin{array}{c} i \\ 1 \\ -2 \end{array} \right|_l + 8 \left| \begin{array}{c} i \\ 1 \\ -2 \end{array} \right|_j^* \end{aligned} \tag{A2}$$

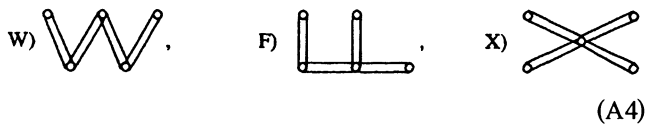
where an asterisk at one of the vertices denotes multiplication by  $\Delta$  with the corresponding index. It is easy to symmetrize the coefficients and sum them in such diagrammatic representations. As a result, for the coefficients with five indices we obtain

$$\begin{aligned}
 C_5(ijkl) &= \frac{490}{3} \left[ \begin{array}{c} + \\ | \\ 1 \quad 1 \\ | \\ + \end{array} \right] \left[ \begin{array}{c} + \\ | \\ 1 \quad 1 \\ | \\ + \end{array} \right], \\
 C_{32}(qj,ilk) &= \frac{56}{3} \left[ \begin{array}{c} + \\ | \\ -13 \quad 5 \\ | \\ z \end{array} \right] \left[ \begin{array}{c} + \\ | \\ 1 \quad 1 \\ | \\ + \end{array} \right] + \frac{28}{3} \left[ \begin{array}{c} z \\ | \\ 16 \quad 25 \\ | \\ z \end{array} \right] \left[ \begin{array}{c} + \\ | \\ 1 \quad 1 \\ | \\ + \end{array} \right] \\
 &\quad - 56 \left( \left[ \begin{array}{c} + \\ | \\ -2 \quad 7 \\ | \\ z \end{array} \right] \left[ \begin{array}{c} + \\ | \\ 1 \quad 0 \\ | \\ + \end{array} \right] + 2 \left[ \begin{array}{c} + \\ | \\ -5 \quad 4 \\ | \\ z \end{array} \right] \left[ \begin{array}{c} + \\ | \\ 0 \quad 1 \\ | \\ + \end{array} \right] \right), \\
 C_{33}(i,jkql) &= -\frac{56}{3} \left[ \begin{array}{c} + \\ | \\ 1 \quad 1 \\ | \\ + \end{array} \right] \left[ \begin{array}{c} + \\ | \\ 47 \quad -7 \\ | \\ - \end{array} \right] + \frac{2}{3} \left[ \begin{array}{c} + \\ | \\ 161 \quad -91 \\ | \\ + \end{array} \right] \left[ \begin{array}{c} + \\ | \\ 1 \quad 1 \\ | \\ + \end{array} \right], \\
 C_{14}(i,qljk) &= \frac{2}{3} \left[ \begin{array}{c} z \\ | \\ 11 \quad 173 \\ | \\ z \end{array} \right] \left[ \begin{array}{c} z \\ | \\ 1 \quad 1 \\ | \\ + \end{array} \right] + 8 \left[ \begin{array}{c} z \\ | \\ 1 \quad -11 \\ | \\ z \end{array} \right] \left[ \begin{array}{c} z \\ | \\ -2 \quad 1 \\ | \\ + \end{array} \right], \\
 C_{15}(i,jk,ql) &= 24 \left[ \begin{array}{c} - \\ | \\ 2 \quad 13 \\ | \\ z \end{array} \right] \left[ \begin{array}{c} + \\ | \\ 0 \quad 1 \\ | \\ + \end{array} \right] + 48 \left[ \begin{array}{c} - \\ | \\ 11 \quad -2 \\ | \\ z \end{array} \right] \left[ \begin{array}{c} + \\ | \\ 0 \quad 1 \\ | \\ + \end{array} \right] \\
 &\quad + 16 \left[ \begin{array}{c} - \\ | \\ 1 \quad -5 \\ | \\ + \end{array} \right] \left[ \begin{array}{c} z \\ | \\ 0 \quad 1 \\ | \\ + \end{array} \right] + 16 \left[ \begin{array}{c} - \\ | \\ -32 \quad 34 \\ | \\ + \end{array} \right] \left[ \begin{array}{c} z \\ | \\ 0 \quad 1 \\ | \\ + \end{array} \right] \\
 &\quad + 4 \cdot \frac{7^2}{3} \left[ \begin{array}{c} z \\ | \\ 1 \quad 1 \\ | \\ + \end{array} \right] \left[ \begin{array}{c} z \\ | \\ 1 \quad 1 \\ | \\ + \end{array} \right] \\
 &\quad + 12 \left[ \begin{array}{c} z \\ | \\ 1 \quad -11 \\ | \\ + \end{array} \right] \left[ \begin{array}{c} z \\ | \\ -3 \quad 5 \\ | \\ + \end{array} \right] + \frac{4}{3} \left[ \begin{array}{c} + \\ | \\ 121 \quad -41 \\ | \\ + \end{array} \right] \left[ \begin{array}{c} z \\ | \\ 0 \quad 1 \\ | \\ z \end{array} \right] \\
 &\quad + \frac{4^2}{3} \left[ \begin{array}{c} + \\ | \\ 29 \quad -52 \\ | \\ + \end{array} \right] \left[ \begin{array}{c} z \\ | \\ 0 \quad 1 \\ | \\ z \end{array} \right] \\
 &\quad + \frac{16}{3} \left[ \begin{array}{c} z \\ | \\ -41 \quad -23 \\ | \\ - \end{array} \right] \left[ \begin{array}{c} z \\ | \\ 1 \quad 0 \\ | \\ + \end{array} \right] + \frac{16}{3} \left[ \begin{array}{c} z \\ | \\ 94 \quad -104 \\ | \\ - \end{array} \right] \left[ \begin{array}{c} z \\ | \\ 0 \quad 0 \\ | \\ + \end{array} \right] \\
 &\quad + \frac{8}{3} \left[ \begin{array}{c} - \\ | \\ 173 \quad -187 \\ | \\ + \end{array} \right] \left[ \begin{array}{c} z \\ | \\ 0 \quad 1 \\ | \\ + \end{array} \right] + \frac{32}{3} \left[ \begin{array}{c} - \\ | \\ -35 \quad -26 \\ | \\ + \end{array} \right] \left[ \begin{array}{c} z \\ | \\ 0 \quad 1 \\ | \\ z \end{array} \right],
 \end{aligned}$$

$$\begin{aligned}
C_{16}(ik, jql) = & \frac{8}{3} \left[ \begin{array}{c} - \\ + \end{array} \left| \begin{array}{c} -167 \\ -41 \end{array} \right. \begin{array}{c} 31 \\ 10 \\ 10 \end{array} \right] + \frac{16}{3} \left[ \begin{array}{c} - \\ + \end{array} \left| \begin{array}{c} -5 \\ 121 \end{array} \right. \begin{array}{c} 239 \\ 0 \\ 1 \\ 0 \end{array} \right] \\
& + \frac{4}{3} \left[ \begin{array}{c} + \\ - \end{array} \left| \begin{array}{c} 1 \\ 1 \end{array} \right. \begin{array}{c} 77 \\ 203 \\ 203 \end{array} \right] + \frac{8}{3} \left[ \begin{array}{c} - \\ + \end{array} \left| \begin{array}{c} 29 \\ 569 \end{array} \right. \begin{array}{c} 317 \\ 1 \\ 0 \\ 0 \end{array} \right] \\
& + \frac{8}{3} \left[ \begin{array}{c} - \\ + \end{array} \left| \begin{array}{c} 173 \\ -151 \end{array} \right. \begin{array}{c} -403 \\ 0 \\ 1 \\ 1 \end{array} \right].
\end{aligned} \tag{A3}$$

Here, at the vertices we indicate the form of the operator, viz.,  $I_i^+$ ,  $I_i^-$  or  $I_i^z$  corresponding to the respective vertex in the operator expression instead of the lattice indices, since after symmetrization the indices referring to the same operators can be positioned arbitrarily. The explicit forms of the coefficients in terms of the diagrams are written out according to the same rules as in (A1). However, now we have a product of two sums for two triangles, and this product has been symmetrized with respect to lattice indices referring to identical operators. The coefficients for  $\mathcal{H}_{ee}^m(p)$  are distinguished by the replacement of each plus sign by a minus sign and of each minus sign by a plus sign in the diagrams.

When the trace is taken in (2.15), the vertices with conjugate operators should be joined in pairs in all possible ways in the coefficients (A3) for  $\mathcal{H}_{ee}^m(p)$  and  $\mathcal{H}_{ee}^{-m}(p)$  (we multiply the coefficients at the vertices) and divide by the number of such ways. This gives the sum of all the possible products of the eight coefficients  $b_{ij}$  (just as the sum of the products of six such coefficients was formed in Sec. 3). In the approximation of infinite-dimensional lattices<sup>19,21</sup> we retain only the ones which do not contain coupling loops. They are:



Loop formation can be avoided only if the vertices common to two triangles are joined to one another in the coefficients for  $m$  and  $-m$ . Furthermore, operators belonging to identical triangles should be paired (triangle to triangle) to find the ‘‘W’’ and ‘‘F’’ contributions, while the ‘‘X’’ contribution forms when all the operators are paired independently of their assignment to triangles.

After summation over the lattice indices, each diagram (A4) gives a multiplier  $B^4$ , since in the approximation of infinite-dimensional lattices, we neglect the sums with a small number of summations appearing because of the need in (A4) to eliminate the terms with coinciding lattice indices.

The expression for  $M_2(m, n)$  presented in Table II is obtained after summing the numerical coefficients in the form of the diagrams (A4) found according to the rules described and multiplying by the numerical coefficient appearing in (4.3) in front of the corresponding correlation function.

Let us move on to coefficients with three lattice indices. In the case of  $\{jk, i\}$  in (A2) the triangles touch along one side, on which one of the vertices has no operator (the free vertex  $l$ ). The three other vertices with operators should be joined in pairs to calculate the trace of (2.15). The formation of coupling loops on the lattice can be avoided only if a product, for example,  $b_{il}b_{ij}$ , with a free vertex at an end and with one coupling ( $b_{il}$ ) along the common side of the triangle is taken in each triangle. Then the summation over the free vertex gives the multiplier  $B$ , and the coefficients take on the simple form

$$2\xi^2 \{ \overset{\square}{ijk}, i \} / \omega_2 = E b_{ji} b_{ik} + Q (b_{ik} b_{kj} + b_{ij} b_{jk}), \tag{A5}$$

where

$$E = \frac{49B}{3\omega_2(8\omega_e)^2} + \frac{3\eta_i}{4\omega_2}, \quad Q = \frac{B}{8\omega_2\omega_e^2} + \frac{\eta_i}{4\omega_2}.$$

We note that in the contributions from the nonuniformity of the rf field we took  $\eta_i = \eta_j$ , since the  $\eta_i$  vary over macroscopic distances. The frequency shift, which is identical for all spins, is assumed to be included in  $\omega_e$ .

The first two terms in the coefficient  $[ijk]$  (A2) have one less summation over the lattice indices and should be omitted in the limit  $d \rightarrow \infty$ . For the other two we find, as in the preceding case,

$$2\xi^2 \{ \overset{\square}{ijk} \} / \omega_2 = D (b_{ji} b_{ik} + b_{ik} b_{kj} + b_{ij} b_{jk}) / 3, \tag{A6}$$

where

$$D = \frac{B}{32\omega_2\omega_e^2} - \frac{\eta_i}{2\omega_2}.$$

After forming the combinations of (A5) and (A6) listed in Table II and substituting them into (4.4), we find

$$\begin{aligned} C_{12}(0) &= B^2(E^2 + 2Q^2), \\ C_{13}(0) &= 4B^2(E^2 + 2Q^2) - B^2(E + 2Q - D)^2 + 4B^2D^2, \\ C_{31}(0) &= B^2(E + 2Q - D)^2/3. \end{aligned} \quad (\text{A7})$$

These expressions should be averaged over the nonuniformity of the rf field. The term that is linear in  $\eta_i$  vanishes. Only the quadratic expression appearing in Eqs. (A7) in the form of a separate term remains. After multiplying through by the coefficients in (4.3), we obtain the result presented in the last column of Table II.

- <sup>1</sup>S. P. Gabuda and A. G. Lundin, *Internal Mobility in Solids* [in Russian] (Nauka, Novosibirsk, 1986).  
<sup>2</sup>U. Haebleren, *High Resolution NMR in Solids* (Academic Press, New York, 1976); M. Mehring, *High Resolution NMR Spectroscopy in Solids* (Springer-Verlag, Berlin-Heidelberg, New York, 1976) [Russ. transl., Mir, Moscow, 1980].  
<sup>3</sup>R. R. Ernst, G. Bodenhausen, and A. Wokaun, *Principles of Nuclear Magnetic Resonance in One and Two Dimensions* (Clarendon Press, Oxford, 1987) [Russ. transl., Mir, Moscow, 1990].  
<sup>4</sup>M. Lee and W. I. Goldberg, *Phys. Rev. A* **140**, 1261 (1965).  
<sup>5</sup>V. E. Zobov and A. V. Ponomarenko, in *Solid-State Radio-Frequency Spectroscopy* [in Russian] (Inst. Fiz. Sibirsk. Otd. Russ. Akad. Nauk, Krasnoyarsk, 1979), p. 70; *Polym. Bull.* **5**, 347 (1981).  
<sup>6</sup>V. A. Atsarkin and T. N. Khazanovich, *Zh. Éksp. Teor. Fiz.* **87**, 279 (1984) [Sov. Phys. JETP **60**, 162 (1984)].

- <sup>7</sup>V. E. Zobov and A. V. Ponomarenko, Preprint No. 657F, Inst. Fiz. Sibirsk. Otd. Russ. Akad. Nauk (1990).  
<sup>8</sup>D. Gamliel, Z. Luz, and S. Vega, *J. Chem. Phys.* **88**, 25 (1988).  
<sup>9</sup>W. S. Warren and A. Pines, *J. Am. Chem. Soc.* **103**, 1613 (1981).  
<sup>10</sup>M. Munowitz and M. Mehring, *Solid State Commun.* **64**, 605 (1987).  
<sup>11</sup>A. E. Mefed, V. A. Atsarkin, and M. E. Zhabotinskiĭ, *Zh. Éksp. Teor. Fiz.* **91**, 671 (1986) [Sov. Phys. JETP **64**, 397 (1986)].  
<sup>12</sup>A. E. Mefed and V. A. Atsarkin, *Zh. Éksp. Teor. Fiz.* **74**, 720 (1978) [Sov. Phys. JETP **47**, 378 (1978)].  
<sup>13</sup>V. A. Atsarkin, A. E. Mefed, and M. I. Rodak, *Fiz. Tverd. Tela (Leningrad)* **21**, 2672 (1979) [Sov. Phys. Solid State **21**, 1537 (1979)].  
<sup>14</sup>A. E. Mefed, *Zh. Éksp. Teor. Fiz.* **86**, 302 (1984).  
<sup>15</sup>A. E. Mefed, *Magnetic Resonance and Related Phenomena, Extended Abstracts of the 27th Congress AMPERE*, edited by K. M. Salikhov (1994), p. 826.  
<sup>16</sup>A. E. Mefed, in *Radio-Frequency Spectroscopy* [in Russian] (Perm' Univ., Perm', 1989), p. 90.  
<sup>17</sup>A. K. Hitrin, V. V. Laiko, and B. N. Provotorov, *Phys. Status Solidi B* **126**, 481 (1984).  
<sup>18</sup>W. F. Wurzbach and S. Gade, *Phys. Rev. B* **6**, 1724 (1972).  
<sup>19</sup>V. E. Zobov and M. A. Popov, *Zh. Éksp. Teor. Fiz.* **103**, 2129 (1993) [JETP **76**, 1062 (1993)].  
<sup>20</sup>V. E. Zobov and M. A. Popov, *Zh. Éksp. Teor. Fiz.* **108**, 1450 (1995) [JETP **81**, 795 (1995)].  
<sup>21</sup>V. E. Zobov and M. A. Popov, *Zh. Éksp. Teor. Fiz.* **108**, 324 (1995) [JETP **81**, 175 (1995)].  
<sup>22</sup>N. K. Gaĭsin and K. M. Enikeev, *Fiz. Tverd. Tela (Leningrad)* **30**, 3263 (1988) [Sov. Phys. Solid State **30**, 1877 (1988)].  
<sup>23</sup>T. Y. Hwang and I. J. Lowe, *Phys. Rev. B* **17**, 2845 (1978).

Translated by P. Shelnitz